Supplementary Information

Comparative Study of the Inverse versus Normal Bicontinuous Cubic Phases of the *β*-D-glucopyranoside Water-Driven Self-Assemblies Using Fluorescent Probes

N. Idayu Zahid,[a] Osama K. Abou-Zied, [*b] N. A. Nabila Saari,[a] and Rauzah Hashim[a]

[a]Department of Chemistry, Faculty of Science, University of Malaya, 50603 Kuala Lumpur, Malaysia
[b]Department of Chemistry, Faculty of Science, Sultan Qaboos University, P.O. Box 36, Postal Code 123, Muscat, Sultanate of Oman

*Corresponding Author: Osama K. Abou-Zied (E-mail: abouzied@squ.edu.om)

Table of Contents

^{1}H NMR and ^{13}C NMR data for the *β*-Glc-OC$_{10}$C$_6$ ····· 2

X-ray investigation of *β*-Glc-OC$_{10}$C$_6$ and *β*-Glc-OC$_8$ (Fig. S1) ····· 3

Absorption spectra of HBO in different solvents (Fig. S2) ····· 4

Fluorescence spectra of HBO in different solvents (Fig. S3) ····· 4

Fluorescence decay transients of HBO in lipids (Fig. S4) ····· 5

Fluorescence lifetime measurements of HBO and its derivatives in lipids (Table S1)··· 5

References ····· 5

^{1}H NMR and ^{13}C NMR spectra for the *β*-Glc-OC$_{10}$C$_6$ ····· 6

^{1}H NMR and ^{13}C NMR for the 2-hexyl-decyl-β-D-glucopyranoside, β-Glc-OC$_{10}$C$_{6}$

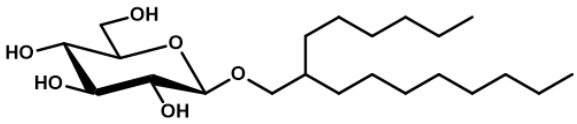

^{1}H NMR (400 MHz, CD_3OD): δ (ppm) = 4.22 (d, 1H, H-1), 3.86 (dd, 1H, H-αa), 3.81 (dd, 1H, H-6a), 3.68 (dd, 1H, H-6b), 3.25-3.41 (m, 4H, H-αb, H-3, H-4, H-5), 3.18 (dd~t, 1H, H-2), 1.60 (m_c, 1H, β-CH_2), 1.29 (m_c, 24H, CH_2), 0.90 (t, 6H, CH_3).

$^{3}J_{1,2}$ = 8.0 Hz, $^{2}J_{6a,6b}$ = 12.0 Hz, $^{2}J_{\alpha a,\alpha b}$ = 12.0 Hz, $^{3}J_{\alpha a,\beta\text{-}CH2}$ = 2.5 Hz.

PENDANT ^{13}C NMR (400 MHz, CD_3OD): δ (ppm) = 103.41 (C-1), 76.81 (C-3), 76.49 (C-4), 73.79 (C-2), 72.68 (C-α), 70.31 (C-5), 61.43 (C-6), 38.22 (CH), 22.46-31.76 (CH_2), 13.23 (CH_3).

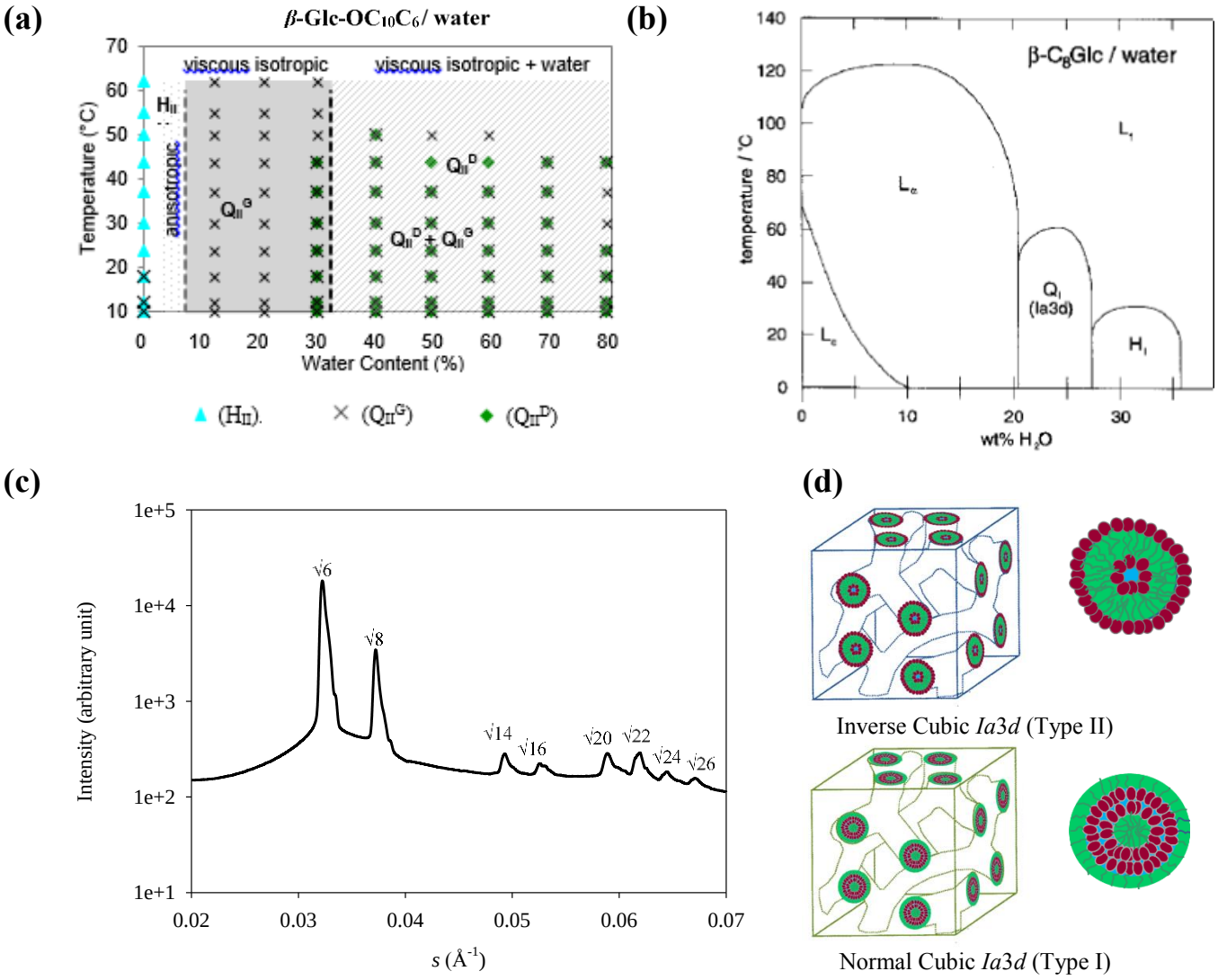

Fig. S1 X-ray investigation of 2-hexyl-decyl-*β*-D-glucopyranoside (*β*-Glc-$OC_{10}C_6$) and octyl-*β*-D-glucopyranoside (*β*-Glc-OC_8): (a) partial binary phase diagram of *β*-Glc-$OC_{10}C_6$, (reprinted with permission from Zahid et al. [1] Copyright (2013) American Chemical Society); (b) binary phase diagram of *β*-Glc-OC_8, (reprinted with permission from Sakya et al. [2] Copyright (1997) Taylor and Francis); (c) small-angle X-ray scattering pattern at 20 % (w/w) water content of *β*-Glc-$OC_{10}C_6$/water system (unpublished result from reference [1]) and (d) schematic cartoon representations of inverse (Type II) and normal (Type I) *Ia3d* bicontinuous cubic phases. In the inverse phase the bicontinuous network region are filled with water while the lipid chains occupy the matrix region. Conversely, in Type I, the network region is hydrophobic, filled with the lipid tails, while the intermediate space is filled with the hydrophilic sugar heads and water.

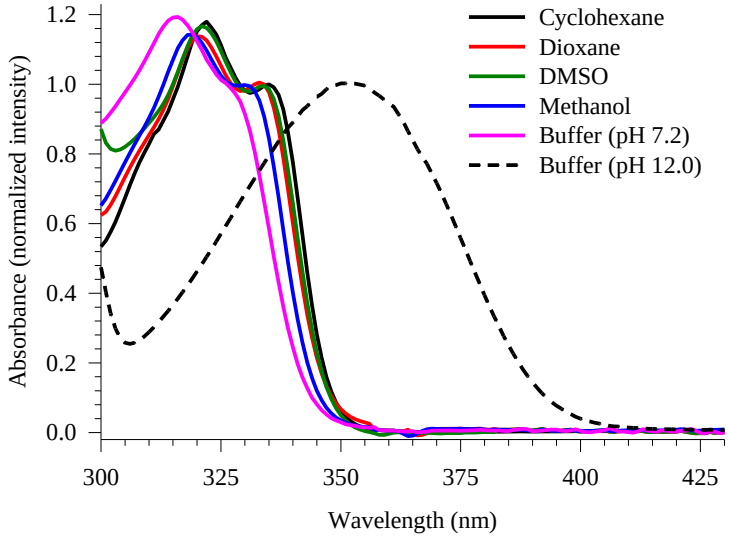

Fig. S2 Absorption spectra of HBO in different solvents, showing the lowest-energy band. Taken from reference [3].

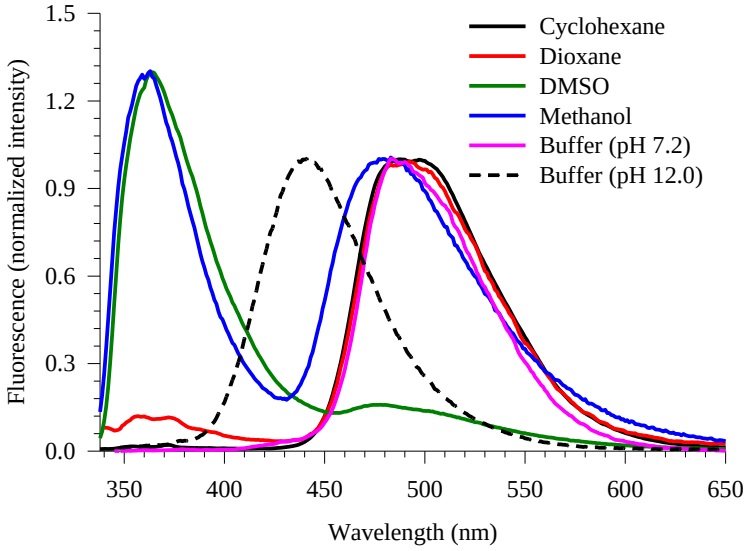

Fig. S3 Fluorescence spectra of HBO in different solvents. λ_{ex} = 330 nm. Taken from reference [3].

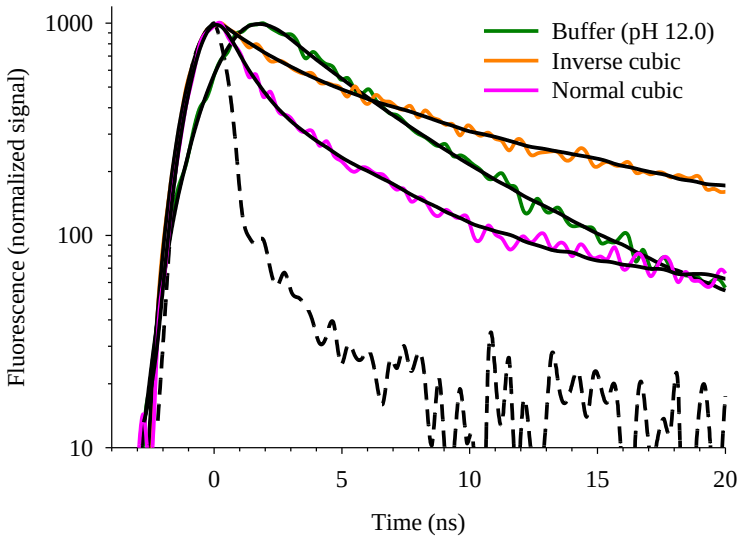

Fig. S4 Fluorescence decay transients of HBO in inverse cubic phase (β-Glc-$OC_{10}C_6$) and normal cubic phase (β-Glc-OC_8). The decay transient of HBO in buffer of pH 12.0 is included for comparison. λ_{ex} = 380 nm. Signal was measured using a 400 nm long-path filter. IRF is shown in a dashed line. Black solid lines represent the best fits.

Table S1. Fluorescence lifetime measurements of HBO and its derivatives in inverse cubic phase (β-Glc-$OC_{10}C_6$) and normal cubic phase (β-Glc-OC_8)

Probe	Lifetime, τ		
	τ_1[a] Keto	τ_2[b] Anion	τ_3[c] Solvated *syn*-enol
Inverse cubic			
HBO		1.6 (0.19)	9.4 (0.81)
HBO-C_4		0.9 (0.30)	6.5 (0.70)
HBO-C_8		1.4 (0.21)	7.2 (0.79)
Normal cubic			
HBO	5.3 (0.58)	0.9 (0.42)	
HBO-C_4	5.2 (0.52)	1.1 (0.48)	
HBO-C_8	5.0 (0.52)	1.0 (0.48)	

Uncertainty in measurements is [a] ± 0.2 ns; [b] ± 0.1 ns; [c] ± 0.2 ns. Relative contributions are listed in parentheses. λ_{ex} = 380 nm. Emission was detected using a 400 nm long-path filter.

References

[1] N. I. Zahid, C. E. Conn, N. J. Brooks, N. Ahmad, J. M. Seddon and R. Hashim, *Langmuir*, 2013, **29**, 15794–15804.

[2] P. Sakya and J. Seddon, *Liq. Cryst.*, 1997, **23**, 409–424.

[3] O. K. Abou-Zied, N. I. Zahid, M. F. Khyasudeen, D. S. Giera, J. C. Thimm and R. Hashim, *Sci. Rep.*, 2015, **5**, 8699.

^{1}H NMR

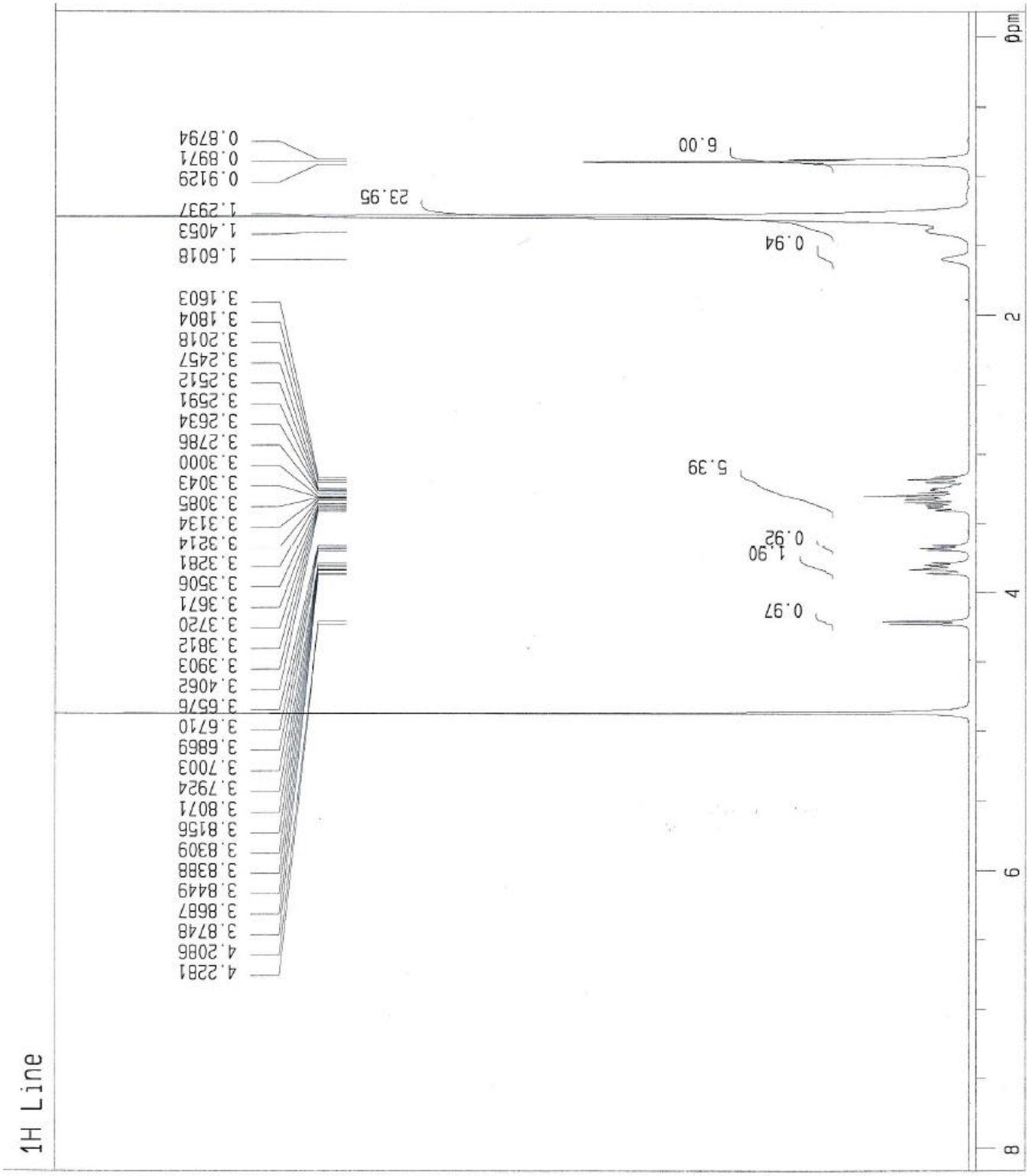
1H Line
ppm
8
6
4
2
0
6.00
23.95
0.94
5.39
0.92
1.90
0.97
0.8794
0.8971
0.9129
1.2937
1.4053
1.6018
3.1603
3.1804
3.2018
3.2457
3.2512
3.2591
3.2634
3.2786
3.3000
3.3043
3.3085
3.3134
3.3214
3.3281
3.3506
3.3671
3.3720
3.3812
3.3903
3.4062
3.6576
3.6710
3.6869
3.7003
3.7924
3.8071
3.8156
3.8309
3.8388
3.8449
3.8687
3.8748
4.2086
4.2281

PENDANT ^{13}C NMR